

## Supporting Information

# Ce<sub>3</sub>F<sub>4</sub>(SO<sub>4</sub>)<sub>4</sub>: Cationic Framework Assembly for Designing Polar Nonlinear Optical Material through Fluorination Degree Modulation

Tianhui Wu,<sup>a,†</sup> Xingxing Jiang,<sup>b,‡</sup> Chao Wu,<sup>a,‡</sup> Zheshuai Lin,<sup>b</sup> Zhipeng Huang,<sup>a</sup> Mark G. Humphrey,<sup>c</sup> and Chi Zhang<sup>a,\*</sup>

<sup>a</sup> *China-Australia Joint Research Center for Functional Molecular Materials, School of Chemical Science and Engineering, Tongji University, Shanghai 200092, China E-mail: chizhang@tongji.edu.cn*

<sup>b</sup> *Technical Institute of Physics and Chemistry, Chinese Academy of Sciences, Beijing 100190, China*

<sup>c</sup> *Research School of Chemistry, Australian National University, Canberra, ACT 2601, Australia*

## Table of Contents

### Theoretical Calculations

**Table S1.** Selected bond distances ( $\text{\AA}$ ) and angles (deg.) for  $\text{Ce}_2\text{F}_2(\text{SO}_4)_3 \cdot 2\text{H}_2\text{O}$ .

**Table S2.** Selected bond distances ( $\text{\AA}$ ) and angles (deg.) for  $\text{Ce}_3\text{F}_4(\text{SO}_4)_4$ .

**Table S3.** Hydrogen-bond interactions of  $\text{Ce}_2\text{F}_2(\text{SO}_4)_3 \cdot 2\text{H}_2\text{O}$ .

**Table S4.** Atomic coordinates ( $\times 10^4$ ), equivalent isotropic displacement parameters ( $\text{\AA}^2 \times 10^3$ ), and the bond valence sum for each atom in the asymmetric unit of  $\text{Ce}_2\text{F}_2(\text{SO}_4)_3 \cdot 2\text{H}_2\text{O}$ .  $U(\text{eq})$  is defined as one third of the trace of the orthogonalized  $U_{ij}$  tensor

**Table S5.** Atomic coordinates ( $\times 10^4$ ), equivalent isotropic displacement parameters ( $\text{\AA}^2 \times 10^3$ ), and the bond valence sum for each atom in the asymmetric unit of  $\text{Ce}_3\text{F}_4(\text{SO}_4)_4$ .  $U(\text{eq})$  is defined as one third of the trace of the orthogonalized  $U_{ij}$  tensor.

**Table S6.** Direction and magnitude of the dipole moments in  $\text{Ce}_3\text{F}_4(\text{SO}_4)_4$ .

**Figure S1.** Experimental and simulated powder X-ray diffraction patterns of  $\text{Ce}_2\text{F}_2(\text{SO}_4)_3 \cdot 2\text{H}_2\text{O}$  (a) and  $\text{Ce}_3\text{F}_4(\text{SO}_4)_4$  (b).

**Figure S2.** SEM images of  $\text{Ce}_2\text{F}_2(\text{SO}_4)_3 \cdot 2\text{H}_2\text{O}$  (a) and  $\text{Ce}_3\text{F}_4(\text{SO}_4)_4$  (b) and their elemental distribution maps.

**Figure S3.** Asymmetric units of  $\text{Ce}_2\text{F}_2(\text{SO}_4)_3 \cdot 2\text{H}_2\text{O}$  (a) and  $\text{Ce}_3\text{F}_4(\text{SO}_4)_4$  (b).

**Figure S4.** Coordination environment of the  $[\text{SO}_4]$  groups in  $\text{Ce}_2\text{F}_2(\text{SO}_4)_3 \cdot 2\text{H}_2\text{O}$ .

**Figure S5.** View of the arrangement between  $[\text{SO}_4]$  groups and Ce-centered polyhedra in  $\text{Ce}_3\text{F}_4(\text{SO}_4)_4$ .

**Figure S6.** Thermogravimetric analyses of  $\text{Ce}_2\text{F}_2(\text{SO}_4)_3 \cdot 2\text{H}_2\text{O}$  (a) and  $\text{Ce}_3\text{F}_4(\text{SO}_4)_4$  (b) under a  $\text{N}_2$  atmosphere.

**Figure S7.** Powder X-ray diffraction patterns for the thermal decomposition residues of  $\text{Ce}_2\text{F}_2(\text{SO}_4)_3 \cdot 2\text{H}_2\text{O}$  (a) and  $\text{Ce}_3\text{F}_4(\text{SO}_4)_4$  (b).

**Figure S8.** Infrared spectra of  $\text{Ce}_2\text{F}_2(\text{SO}_4)_3 \cdot 2\text{H}_2\text{O}$  (a) and  $\text{Ce}_3\text{F}_4(\text{SO}_4)_4$  (b).

**Figure S9** UV-Vis-NIR diffuse absorption spectra of  $\text{Ce}_2\text{F}_2(\text{SO}_4)_3 \cdot 2\text{H}_2\text{O}$  (a) and  $\text{Ce}_3\text{F}_4(\text{SO}_4)_4$  (b). The inset shows the corresponding band gap.

**Figure S10.** Comparison of (a) the original crystal, and the crystal achieving complete extinction of  $\text{Ce}_3\text{F}_4(\text{SO}_4)_4$  under positive (b), and negative (c) rotation of compensatory. (d) Thickness of the  $\text{Ce}_3\text{F}_4(\text{SO}_4)_4$  crystal.

**Figure S11** Calculated band structure of  $\text{Ce}_3\text{F}_4(\text{SO}_4)_4$ .

**Figure S12.** The calculated birefringence dispersion curve of  $\text{Ce}_3\text{F}_4(\text{SO}_4)_4$ .

### References

## Theoretical Calculations:

First-principles simulations were performed using CASTEP,<sup>S1</sup> a plane-wave pseudopotential total energy package based on density functional theory (DFT).<sup>S2, S3</sup> The functional developed by Perdew, Burke and Ernzerhof (PBE)<sup>S4</sup> in the generalized gradient approximation (GGA)<sup>S5</sup> form was adopted to describe the exchange-correlation energy. The optimized norm-conserving pseudopotential<sup>S6</sup> for Ce, S, F, and O allowed us to use a small plane-wave basis set without compromising the accuracy required for the calculations. A kinetic energy cutoff of 900 eV and Monkhorst-Pack<sup>S7</sup> k-point mesh spanning less than 0.03 Å<sup>-1</sup> in the Brillouin zone were chosen.

The bandgap calculated by standard DFT is smaller than the experimental data due to the discontinuity in the exchange-correlation functional, so a scissor operator<sup>S8</sup> was used to shift the conduction band upward to agree with the measured data. The imaginary part of the dielectric function of the electronic transition between the valence band (VB) and the conduction band (CB) was calculated from the scissor-operator-corrected electronic band structure. The real part of the dielectric function, i.e., the refractive indices, was then determined by a Kramers-Kronig transform.<sup>S9</sup> The anisotropic SHG coefficients were calculated using a program developed by our group.<sup>S10, S11</sup> In the SHG-weighted electron density analysis, the electron density of all the orbitals is summed by a weight positively correlated with its contribution to the SHG coefficient, and thus the electronic cloud of orbitals crucial to the SHG response is highlighted in real space.<sup>S12</sup>

**Table S1.** Selected bond distances ( $\text{\AA}$ ) and angles (deg.) for  $\text{Ce}_2\text{F}_2(\text{SO}_4)_3 \cdot 2\text{H}_2\text{O}$  <sup>[a]</sup>.

Ce(1)-F(1)#1	2.194(2)	O(4)#2-Ce(1)-O(1)	76.20(10)
Ce(1)-O(5)	2.220(3)	O(2)#3-Ce(1)-O(1)	77.61(9)
Ce(1)-F(1)	2.242(2)	F(1)#1-Ce(1)-O(3)#4	69.57(9)
Ce(1)-O(4)#2	2.282(3)	O(5)-Ce(1)-O(3)#4	75.06(11)
Ce(1)-O(2)#3	2.314(3)	F(1)-Ce(1)-O(3)#4	72.50(9)
Ce(1)-O(1)	2.379(3)	O(4)#2-Ce(1)-O(3)#4	73.25(10)
Ce(1)-O(3)#4	2.381(3)	O(2)#3-Ce(1)-O(3)#4	140.49(10)
Ce(1)-O(1W)	2.394(3)	O(1)-Ce(1)-O(3)#4	121.91(10)
S(1)-O(3)	1.459(3)	F(1)#1-Ce(1)-O(1W)	83.28(10)
S(1)-O(1)	1.468(3)	O(5)-Ce(1)-O(1W)	71.64(11)
S(1)-O(4)	1.471(3)	F(1)-Ce(1)-O(1W)	117.76(10)
S(1)-O(2)	1.475(3)	O(4)#2-Ce(1)-O(1W)	144.75(10)
S(2)-O(6)#5	1.447(3)	O(2)#3-Ce(1)-O(1W)	75.58(10)
S(2)-O(6)	1.447(3)	O(1)-Ce(1)-O(1W)	73.95(10)
S(2)-O(5)	1.488(3)	O(3)#4-Ce(1)-O(1W)	139.74(10)
S(2)-O(5)#5	1.488(3)	O(3)-S(1)-O(1)	111.48(16)
F(1)-Ce(1)#4	2.194(2)	O(3)-S(1)-O(4)	110.05(17)
O(1W)-H(1)	0.8186	O(1)-S(1)-O(4)	108.63(16)
O(1W)-H(2)	0.8194	O(3)-S(1)-O(2)	108.55(17)
O(2)-Ce(1)#6	2.314(3)	O(1)-S(1)-O(2)	109.73(16)
O(3)-Ce(1)#1	2.381(3)	O(4)-S(1)-O(2)	108.36(16)
O(4)-Ce(1)#7	2.282(3)	O(6)#5-S(2)-O(6)	113.7(3)
		O(6)#5-S(2)-O(5)	109.90(18)
F(1)#1-Ce(1)-O(5)	80.90(10)	O(6)-S(2)-O(5)	108.92(18)
F(1)#1-Ce(1)-F(1)	138.66(3)	O(6)#5-S(2)-O(5)#5	108.92(18)
O(5)-Ce(1)-F(1)	74.00(10)	O(6)-S(2)-O(5)#5	109.90(18)
F(1)#1-Ce(1)-O(4)#2	105.26(9)	O(5)-S(2)-O(5)#5	105.2(3)
O(5)-Ce(1)-O(4)#2	142.88(11)	Ce(1)#4-F(1)-Ce(1)	161.28(12)
F(1)-Ce(1)-O(4)#2	78.42(10)	S(1)-O(1)-Ce(1)	141.43(16)
F(1)#1-Ce(1)-O(2)#3	147.28(9)	Ce(1)-O(1W)-H(1)	118.1
O(5)-Ce(1)-O(2)#3	114.60(11)	Ce(1)-O(1W)-H(2)	125.3
F(1)-Ce(1)-O(2)#3	73.97(9)	H(1)-O(1W)-H(2)	116.2
O(4)#2-Ce(1)-O(2)#3	80.10(10)	S(1)-O(2)-Ce(1)#6	145.50(17)
F(1)#1-Ce(1)-O(1)	72.66(9)	S(1)-O(3)-Ce(1)#1	141.27(17)
O(5)-Ce(1)-O(1)	138.50(10)	S(1)-O(4)-Ce(1)#7	163.18(18)
F(1)-Ce(1)-O(1)	144.56(9)	S(2)-O(5)-Ce(1)	155.4(2)

<sup>[a]</sup> Symmetry codes for  $\text{Ce}_2\text{F}_2(\text{SO}_4)_3 \cdot 2\text{H}_2\text{O}$ : #1 x, -y-1, z+1/2; #2 -x-1/2, -y-1, z-1/2; #3 x, -y, z-1/2; #4 x, -y-1, z-1/2; #5 -x, y, -z+1/2; #6 x, -y, z+1/2; #7 -x-1/2, -y-1, z+1/2.

**Table S2.** Selected bond distances ( $\text{\AA}$ ) and angles (deg.) for  $\text{Ce}_3\text{F}_4(\text{SO}_4)_4$  [a].

Ce(1)-F(1)	2.239(6)	O(2)#2-Ce(1)-O(7)	69.83(18)
Ce(1)-F(1)#1	2.251(6)	F(2)-Ce(1)-O(7)	126.33(15)
Ce(1)-O(1)	2.256(5)	O(8)-Ce(1)-O(7)	133.3(2)
Ce(1)-O(2)#2	2.284(5)	O(6)-Ce(1)-O(7)	137.7(2)
Ce(1)-F(2)	2.293(4)	F(2)#3-Ce(2)-F(2)#4	118.0(2)
Ce(1)-O(8)	2.311(6)	F(2)#3-Ce(2)-O(5)#5	142.72(16)
Ce(1)-O(6)	2.365(6)	F(2)#4-Ce(2)-O(5)#5	76.79(18)
Ce(1)-O(7)	2.395(4)	F(2)#3-Ce(2)-O(5)	76.79(18)
Ce(2)-F(2)#3	2.193(4)	F(2)#4-Ce(2)-O(5)	142.72(16)
Ce(2)-F(2)#4	2.193(4)	O(5)#5-Ce(2)-O(5)	113.2(3)
Ce(2)-O(5)#5	2.311(5)	F(2)#3-Ce(2)-O(4)#6	73.26(17)
Ce(2)-O(5)	2.311(5)	F(2)#4-Ce(2)-O(4)#6	73.30(16)
Ce(2)-O(4)#6	2.328(5)	O(5)#5-Ce(2)-O(4)#6	79.86(19)
Ce(2)-O(4)#7	2.328(5)	O(5)-Ce(2)-O(4)#6	142.27(16)
Ce(2)-O(3)#5	2.355(5)	F(2)#3-Ce(2)-O(4)#7	73.30(16)
Ce(2)-O(3)	2.355(5)	F(2)#4-Ce(2)-O(4)#7	73.26(17)
S(1)-O(4)	1.462(4)	O(5)#5-Ce(2)-O(4)#7	142.27(16)
S(1)-O(3)	1.465(5)	O(5)-Ce(2)-O(4)#7	79.86(19)
S(1)-O(1)	1.467(5)	O(4)#6-Ce(2)-O(4)#7	112.1(3)
S(1)-O(2)	1.475(6)	F(2)#3-Ce(2)-O(3)#5	138.81(16)
S(2)-O(7)#7	1.456(5)	F(2)#4-Ce(2)-O(3)#5	75.94(16)
S(2)-O(6)	1.474(8)	O(5)#5-Ce(2)-O(3)#5	75.99(18)
S(2)-O(8)#3	1.465(6)	O(5)-Ce(2)-O(3)#5	72.40(17)
S(2)-O(5)	1.474(5)	O(4)#6-Ce(2)-O(3)#5	144.38(16)
F(1)-Ce(1)#8	2.251(6)	O(4)#7-Ce(2)-O(3)#5	74.90(18)
F(2)-Ce(2)#2	2.193(4)	F(2)#3-Ce(2)-O(3)	75.94(16)
O(2)-Ce(1)#3	2.284(5)	F(2)#4-Ce(2)-O(3)	138.81(16)
O(4)-Ce(2)#9	2.328(5)	O(5)#5-Ce(2)-O(3)	72.40(17)
O(7)-S(2)#9	1.456(5)	O(5)-Ce(2)-O(3)	75.99(18)
O(8)-S(2)#2	1.465(6)	O(4)#6-Ce(2)-O(3)	74.90(18)
		O(4)#7-Ce(2)-O(3)	144.38(16)
F(1)-Ce(1)-F(1)#1	77.54(3)	O(3)#5-Ce(2)-O(3)	120.7(2)
F(1)-Ce(1)-O(1)	83.9(2)	O(4)-S(1)-O(3)	110.5(3)
F(1)#1-Ce(1)-O(1)	144.50(18)	O(4)-S(1)-O(1)	108.9(3)
F(1)-Ce(1)-O(2)#2	142.72(17)	O(3)-S(1)-O(1)	110.1(3)
F(1)#1-Ce(1)-O(2)#2	85.3(2)	O(4)-S(1)-O(2)	108.8(3)
O(1)-Ce(1)-O(2)#2	91.84(18)	O(3)-S(1)-O(2)	110.2(3)
F(1)-Ce(1)-F(2)	139.97(17)	O(1)-S(1)-O(2)	108.2(3)
F(1)#1-Ce(1)-F(2)	137.76(19)	O(7)#7-S(2)-O(6)	108.5(3)

O(1)-Ce(1)-F(2)	72.96(17)	O(7)#7-S(2)-O(8)#3	107.1(4)
O(2)#2-Ce(1)-F(2)	71.65(16)	O(6)-S(2)-O(8)#3	111.4(4)
F(1)-Ce(1)-O(8)	124.7(2)	O(7)#7-S(2)-O(5)	111.0(3)
F(1)#1-Ce(1)-O(8)	70.71(19)	O(6)-S(2)-O(5)	110.0(3)
O(1)-Ce(1)-O(8)	143.2(2)	O(8)#3-S(2)-O(5)	108.8(3)
O(2)#2-Ce(1)-O(8)	78.4(2)	Ce(1)-F(1)-Ce(1)#8	170.0(3)
F(2)-Ce(1)-O(8)	70.25(18)	Ce(2)#2-F(2)-Ce(1)	155.4(2)
F(1)-Ce(1)-O(6)	72.5(2)	S(1)-O(1)-Ce(1)	168.2(4)
F(1)#1-Ce(1)-O(6)	121.8(2)	S(1)-O(2)-Ce(1)#3	151.2(3)
O(1)-Ce(1)-O(6)	79.5(2)	S(1)-O(3)-Ce(2)	144.1(3)
O(2)#2-Ce(1)-O(6)	143.12(19)	S(1)-O(4)-Ce(2)#9	150.8(4)
F(2)-Ce(1)-O(6)	71.54(17)	S(2)-O(5)-Ce(2)	145.8(4)
O(8)-Ce(1)-O(6)	87.3(3)	S(2)-O(6)-Ce(1)	147.1(4)
F(1)-Ce(1)-O(7)	73.60(18)	S(2)#9-O(7)-Ce(1)	143.8(3)
F(1)#1-Ce(1)-O(7)	73.41(18)	S(2)#2-O(8)-Ce(1)	156.2(4)
O(1)-Ce(1)-O(7)	72.43(19)		

[a] Symmetry codes for Ce<sub>3</sub>F<sub>4</sub>(SO<sub>4</sub>)<sub>4</sub>: #1 -x-1/2, y+1/2, -z-1; #2 x, y+1, z; #3 x, y-1, z; #4 -x, y-1, -z; #5 -x, y, -z; #6 -x-1/2, y-1/2, -z; #7 x+1/2, y-1/2, z; #8 -x-1/2, -y-1/2, -z-1; #9 x-1/2, y+1/2, z.

**Table S3.** Hydrogen-bond interactions of Ce<sub>2</sub>F<sub>2</sub>(SO<sub>4</sub>)<sub>3</sub>·2H<sub>2</sub>O.

D—H···A	d(D—H)	d(H···A)	d(D···A)	∠(DHA)
O1W—H1WA···O6	0.8200	2.2000	2.7977	130.00
O1W—H1WB···O6	0.8200	2.0300	2.8014	157.00

**Table S4.** Atomic coordinates ( $\times 10^4$ ), equivalent isotropic displacement parameters ( $\text{\AA}^2 \times 10^3$ ), and the bond valence sum for each atom in the asymmetric unit of  $\text{Ce}_2\text{F}_2(\text{SO}_4)_3 \cdot 2\text{H}_2\text{O}$ .  $U(\text{eq})$  is defined as one third of the trace of the orthogonalized  $U_{ij}$  tensor.

Atom	<i>x</i>	<i>y</i>	<i>z</i>	$U_{\text{eq}}(\text{\AA}^2)$	BVS
Ce(1)	-1444(1)	-3858(1)	2428(1)	6(1)	3.80
S(1)	-1936(1)	-1135(1)	6061(1)	7(1)	6.09
S(2)	0	-6574(2)	2500	13(1)	6.12
F(1)	-1359(1)	-4572(4)	-229(3)	15(1)	1.10
O(1)	-1986(1)	-1894(4)	4387(3)	12(1)	1.91
O(2)	-1598(1)	810(4)	6074(3)	13(1)	1.96
O(3)	-1616(1)	-2582(4)	7104(3)	13(1)	1.95
O(4)	-2556(1)	-761(4)	6693(3)	14(1)	2.02
O(5)	-520(1)	-5196(5)	2104(4)	20(1)	2.04
O(6)	146(2)	-7780(5)	1080(4)	28(1)	1.61
O(1W)	-711(1)	-1581(5)	3597(4)	24(1)	3.22

**Table S5.** Atomic coordinates ( $\times 10^4$ ), equivalent isotropic displacement parameters ( $\text{\AA}^2 \times 10^3$ ), and the bond valence sum for each atom in the asymmetric unit of  $\text{Ce}_3\text{F}_4(\text{SO}_4)_4$ .  $U(\text{eq})$  is defined as one third of the trace of the orthogonalized  $U_{ij}$  tensor.

Atom	x	y	z	$U_{\text{eq}}(\text{\AA}^2)$	BVS
Ce(1)	-1992(1)	4460(1)	-3418(1)	5(1)	3.74
Ce(2)	0	-3064(1)	0	5(1)	3.82
S(1)	-2644(1)	-609(4)	-1419(1)	6(1)	6.11
S(2)	18(1)	-529(4)	-3090(1)	9(1)	6.11
F(1)	-2417(4)	1706(13)	-4903(4)	25(1)	1.02
F(2)	-889(3)	4917(7)	-1552(4)	13(1)	1.03
O(1)	-2483(4)	1572(10)	-2129(5)	16(1)	2.07
O(2)	-2755(4)	-2637(11)	-2298(5)	16(1)	2.00
O(3)	-1692(4)	-983(9)	-466(4)	12(1)	1.95
O(4)	-3674(3)	-387(11)	-841(4)	13(1)	1.99
O(5)	274(4)	-792(12)	-1727(4)	15(1)	1.97
O(6)	-446(4)	1863(16)	-3395(5)	21(1)	1.90
O(7)	-3983(4)	4167(11)	-3707(4)	10(1)	1.95
O(8)	-763(5)	7585(10)	-3558(5)	20(1)	2.00

**Table S6.** Direction and magnitude of the dipole moments in Ce<sub>3</sub>F<sub>4</sub>(SO<sub>4</sub>)<sub>4</sub>.

Species	Dipole moment (D)			
	x (a)-component	y (b)-component	z (c)-component	
[CeO <sub>2</sub> F <sub>6</sub> ]	2.29	0.35	-2.69	
	-2.29	0.35	2.69	
	-1.11	0.17	1.31	
	-1.13	0.17	1.33	
	1.14	0.17	-1.34	
	1.14	0.17	-1.34	
[CeO <sub>3</sub> F <sub>5</sub> ]	0	-0.84	0	
	0	-0.84	0	
	0	-0.42	0	
	0	-0.42	0	
	0	-0.42	0	
	0	-0.42	0	
Ce <sub>3</sub> F <sub>4</sub> (SO <sub>4</sub> ) <sub>4</sub>	0.73	0.13	0.87	
	[S(1)O <sub>4</sub> ]	0.73	0.13	0.87
		-0.73	0.13	-0.87
		-0.73	0.13	-0.87
		0.57	-0.68	-0.18
		-0.57	-0.68	0.18
[S(2)O <sub>4</sub> ]	0.29	-0.34	-0.09	
		0.29	-0.34	-0.09
		-0.29	-0.34	0.09
		-0.29	-0.34	0.09
		0.29	-0.34	-0.09
		-0.29	-0.34	0.09

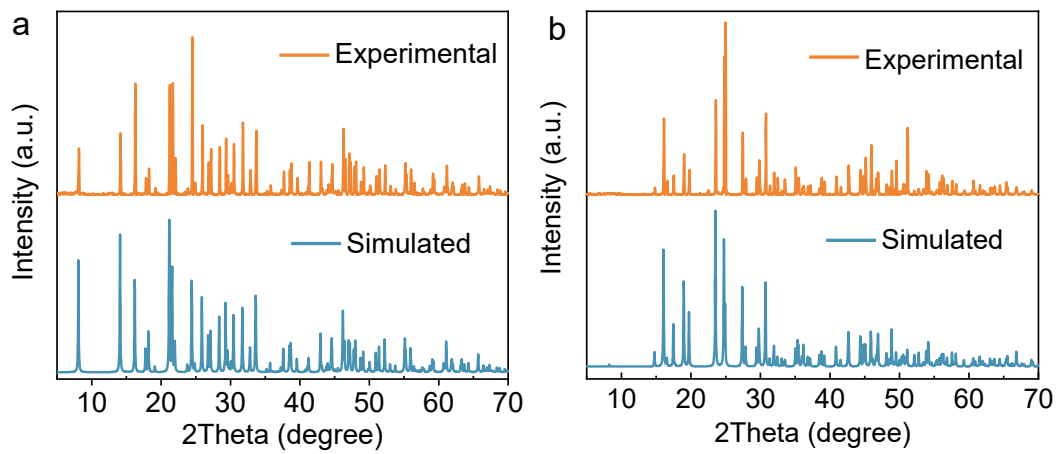


**Figure S1.** Experimental and simulated powder X-ray diffraction patterns of  $\text{Ce}_2\text{F}_2(\text{SO}_4)_3 \cdot 2\text{H}_2\text{O}$  (a) and  $\text{Ce}_3\text{F}_4(\text{SO}_4)_4$  (b).

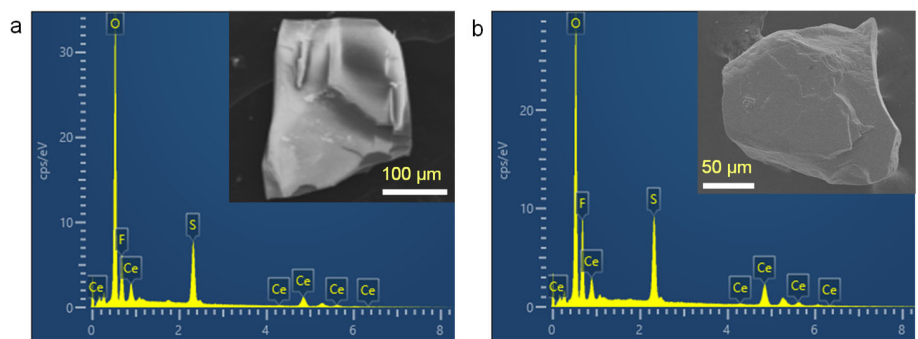


**Figure S2.** SEM images of  $\text{Ce}_2\text{F}_2(\text{SO}_4)_3 \cdot 2\text{H}_2\text{O}$  (a) and  $\text{Ce}_3\text{F}_4(\text{SO}_4)_4$  (b) and their elemental distribution maps.

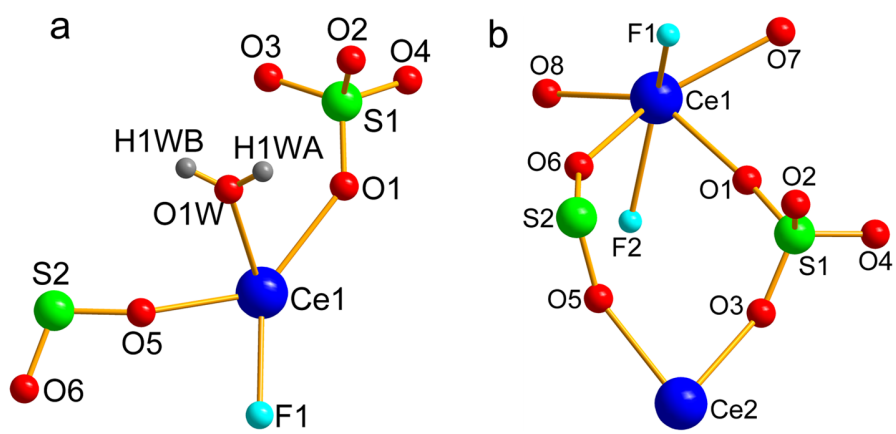


**Figure S3.** Asymmetric units of  $\text{Ce}_2\text{F}_2(\text{SO}_4)_3 \cdot 2\text{H}_2\text{O}$  (a) and  $\text{Ce}_3\text{F}_4(\text{SO}_4)_4$  (b).

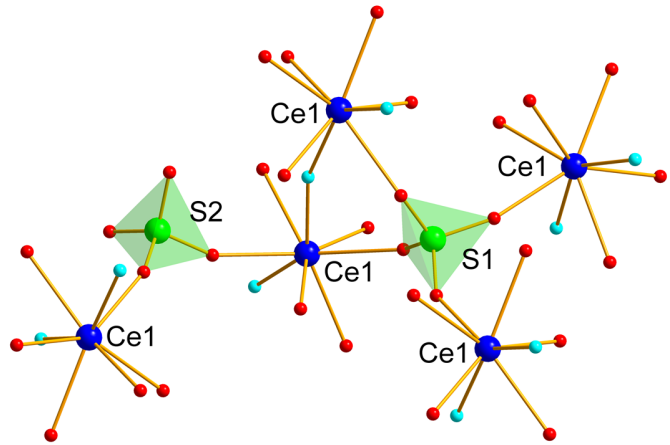


**Figure S4.** Coordination environment of the  $[\text{SO}_4]$  groups in  $\text{Ce}_2\text{F}_2(\text{SO}_4)_3 \cdot 2\text{H}_2\text{O}$ .

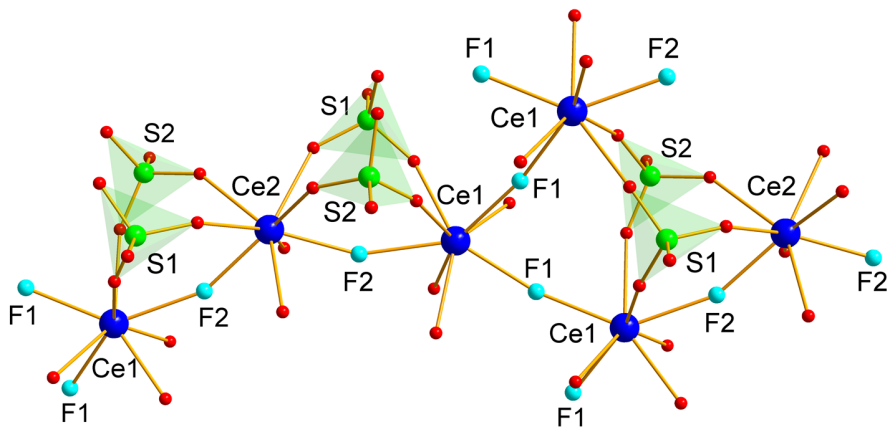


**Figure S5.** View of the arrangement between  $[\text{SO}_4]$  groups and Ce-centered polyhedra in  $\text{Ce}_3\text{F}_4(\text{SO}_4)_4$ .

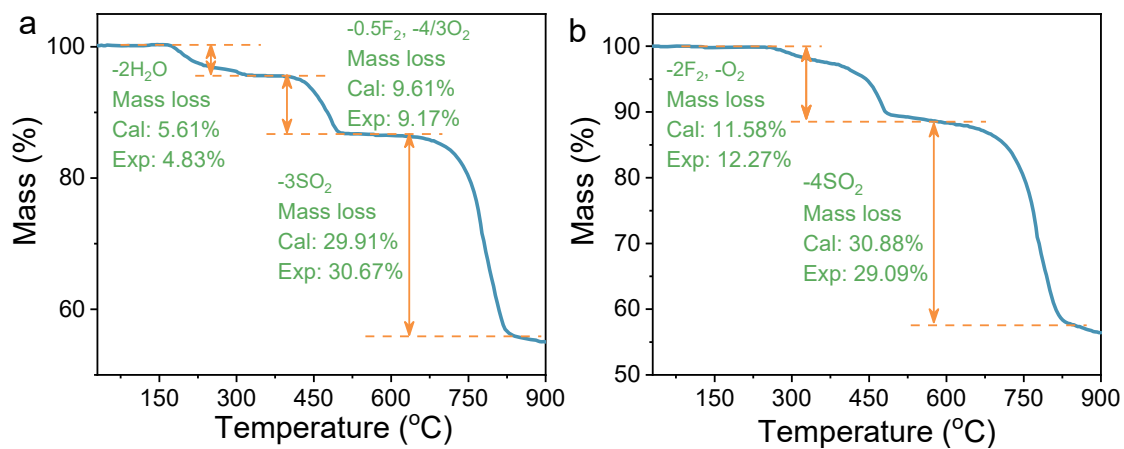


**Figure S6.** Thermogravimetric analyses of  $\text{Ce}_2\text{F}_2(\text{SO}_4)_3 \cdot 2\text{H}_2\text{O}$  (a) and  $\text{Ce}_3\text{F}_4(\text{SO}_4)_4$  (b) under a  $\text{N}_2$  atmosphere.

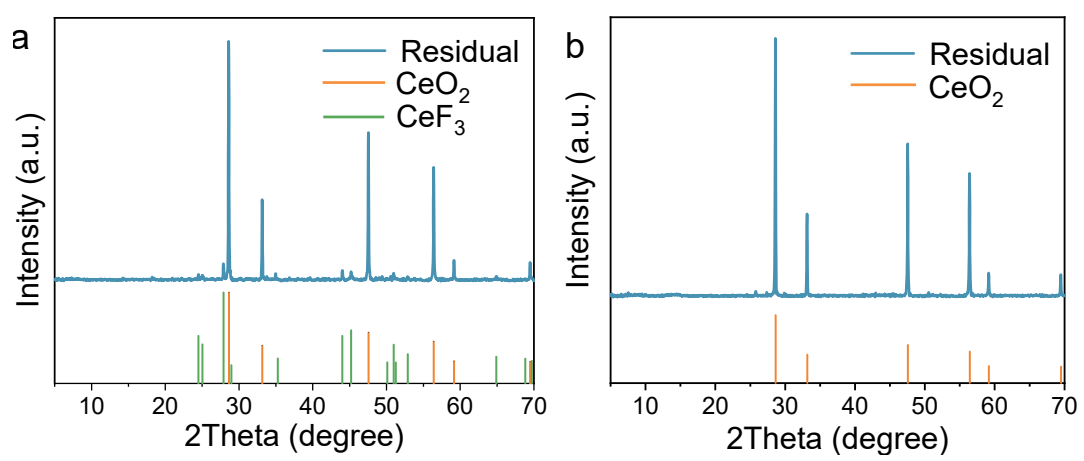


**Figure S7.** Powder X-ray diffraction patterns for the thermal decomposition residues of  $\text{Ce}_2\text{F}_2(\text{SO}_4)_3 \cdot 2\text{H}_2\text{O}$  (a) and  $\text{Ce}_3\text{F}_4(\text{SO}_4)_4$  (b).

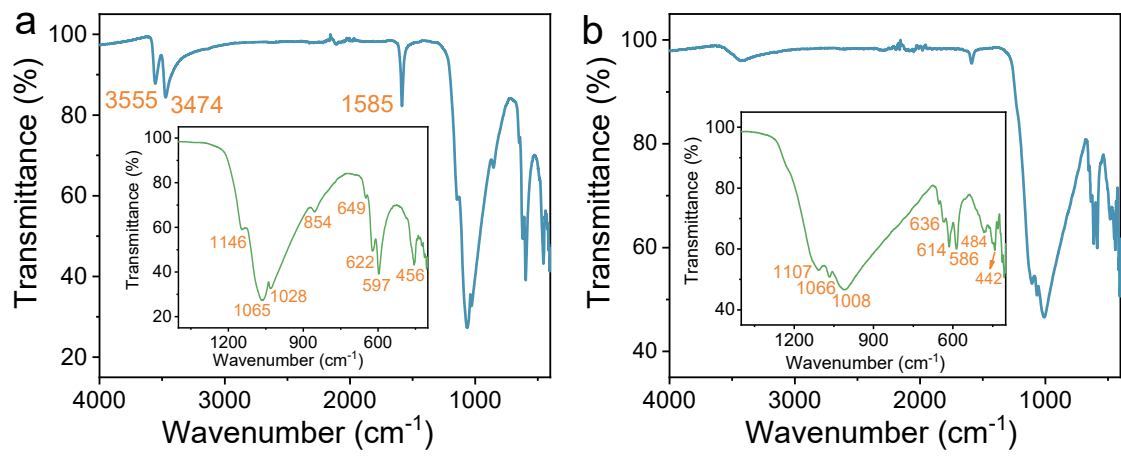


**Figure S8.** Infrared spectra of  $\text{Ce}_2\text{F}_2(\text{SO}_4)_3 \cdot 2\text{H}_2\text{O}$  (a) and  $\text{Ce}_3\text{F}_4(\text{SO}_4)_4$  (b).

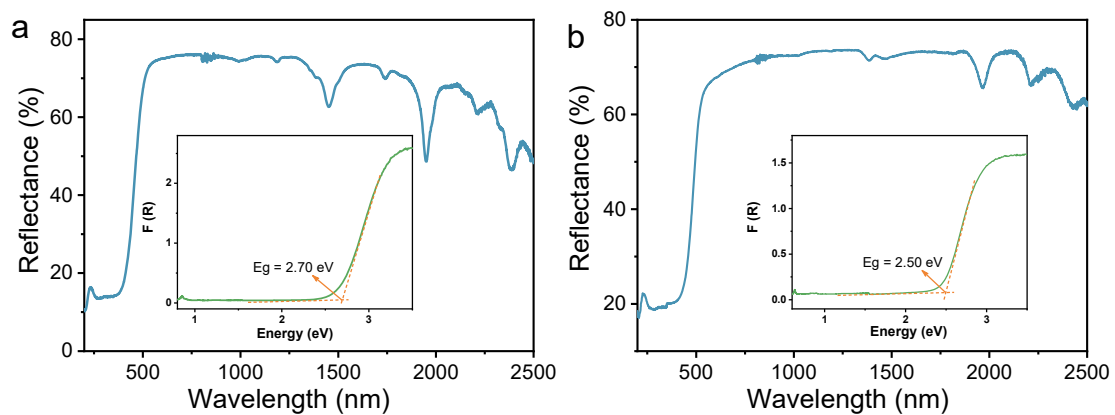


**Figure S9.** UV-Vis-NIR diffuse reflectance spectra of  $\text{Ce}_2\text{F}_2(\text{SO}_4)_3 \cdot 2\text{H}_2\text{O}$  (a) and  $\text{Ce}_3\text{F}_4(\text{SO}_4)_4$  (b). The inset shows the corresponding band gap.

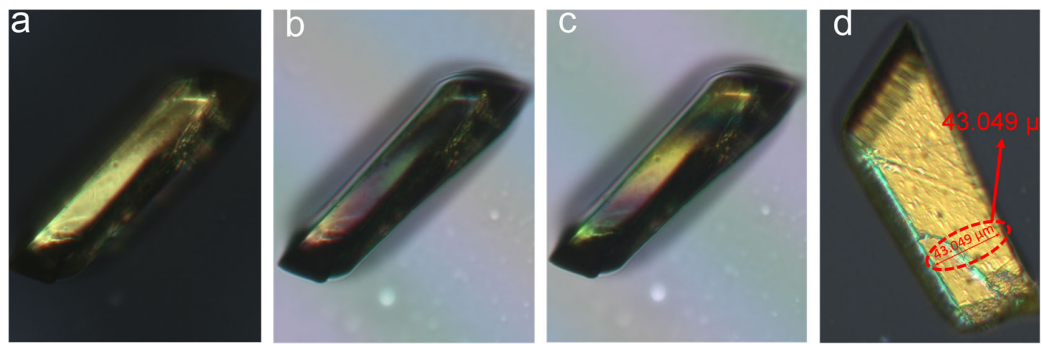


**Figure S10.** Comparison of (a) the original crystal, and the crystal achieving complete extinction of  $\text{Ce}_3\text{F}_4(\text{SO}_4)_4$  under positive (b), and negative (c) rotation of compensatory. (d) Thickness of the  $\text{Ce}_3\text{F}_4(\text{SO}_4)_4$  crystal.

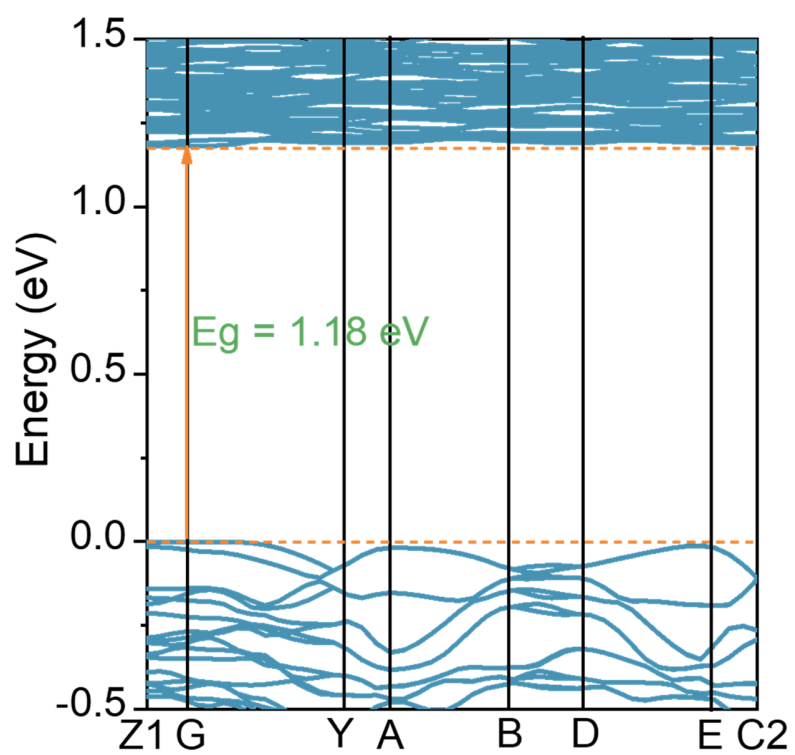


**Figure S11** Calculated band structure of  $\text{Ce}_3\text{F}_4(\text{SO}_4)_4$ .

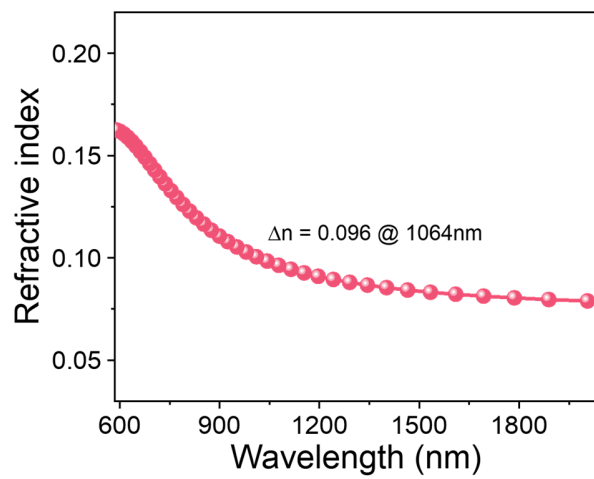


**Figure S12.** The calculated birefringence dispersion curve of  $\text{Ce}_3\text{F}_4(\text{SO}_4)_4$ .

## References

- [S1] S. J. Clark, M. D. Segall, C. J. Pickard, P. J. Hasnip, M. I. J. Probert, K. Refson, M. C. Payne, *Z. Kristallogr.*, **2005**, *220*, 567-570.
- [S2] W. Kohn, L. J. Sham, *Phys. Rev.*, **1965**, *140*, A1133-A1138.
- [S3] M. C. Payne, M. P. Teter, D. C. Allan, T. A. Arias, J. D. Joannopoulos, *Rev. Mod. Phys.*, **1992**, *64*, 1045-1097.
- [S4] J. P. Perdew, K. Burke, M. Ernzerhof, *Phys. Rev. Lett.*, **1996**, *77*, 3865-3868.
- [S5] J. P. Perdew, Y. Wang, *Phys. Rev. B: Condens. Matter Mater. Phys.*, **1992**, *46*, 12947-12954.
- [S6] D. R. Hamann, M. Schluter, C. Chiang, *Phys. Rev. Lett.*, **1979**, *43*, 1494-1497.
- [S7] H. J. Monkhorst, J. D. Pack, *Phys. Rev. B: Solid State*, **1976**, *13*, 5188-5192.
- [S8] R. W. Godby, M. Schluter, L. J. Sham, *Phys. Rev. B: Condens. Matter Mater. Phys.*, **1988**, *37*, 10159-10175.
- [S9] E. D. Palik, *Handbook of Optical Constants of Solids*; Academic: New York, **1985**.
- [S10] Z. S. Lin, X. X. Jiang, L. Kang, P. F. Gong, S. Y. Luo, M. H. Lee, *J. Phys. D: Appl. Phys.*, **2014**, *47*, 253001.
- [S11] J. Lin, M. H. Lee, Z. P. Liu, C. T. Chen, C. J. Pickard, *Phys. Rev. B: Condens. Matter Mater. Phys.*, **1999**, *60*, 13380-13389.
- [S12] M. H. Lee, C. H. Yang and J. H. Jan, *Phys. Rev. B*, **2004**, *70*, 235110-235120.